HHS Public Access

Author manuscript

Cancer Immunol Res. Author manuscript; available in PMC 2020 May 01.

Published in final edited form as:

Cancer Immunol Res. 2019 November ; 7(11): 1824–1836. doi:10.1158/2326-6066.CIR-19-0299.

Single-cell transcriptome analysis reveals gene signatures associated with T-cell persistence following adoptive cell therapy

Yong-Chen Lu[1], **Li Jia**[1], **Zhili Zheng**[1], **Eric Tran**[1,2], **Paul F. Robbins**[1], **Steven A. Rosenberg**[1]

[1]Surgery Branch, National Cancer Institute, National Institutes of Health, Bethesda, MD 20892, USA.

[2]Current address: Earle A. Chiles Research Institute, Providence Cancer Institute, Portland, OR 97213, USA

Abstract

Adoptive cell therapy (ACT) using tumor-infiltrating lymphocytes (TILs) can mediate responses in some patients with metastatic epithelial cancer. Identifying gene signatures associated with successful ACT might enable the development of improved therapeutic approaches. The persistence of transferred T cells in the peripheral blood is one indication of clinical effectiveness, but many T-cell and host factors may influence T-cell persistence. To limit these variables, we previously studied a patient with metastatic colorectal cancer treated with polyclonal TILs targeting the *KRAS*(G12D) hotspot mutation, who experienced a partial response for 9 months. Three dominant clonotypes specifically recognizing KRAS(G12D) epitopes were identified, but we found that only two clonotypes persisted 40 days after ACT. Because of these findings, in this study, we performed the single-cell transcriptome analysis of the infused TILs. The analysis revealed a total of 472 genes that were differentially expressed between clonotypes 9.1-NP and 9.2-P single cells, and 528 genes between 9.1-NP and 10-P. Following these clonotypes in the peripheral blood after ACT, the gene expression patterns changed, but *IL7R*, *ITGB1*, *KLF2* and *ZNF683* remained expressed in the persistent 9.2-P and 10-P cells, compared to the non-persistent 9.1-NP cells. Additionally, four autologous TILs, which were used for treatment but persisted poorly one month after ACT, did not express the gene profiles associated with persistence. These results suggest that certain TIL populations possess a unique gene expression profile that can lead to the persistence of T cells. Thus, this single-patient study provides an insight on how to improve ACT for solid cancer.

Keywords

single-cell; adoptive cell therapy; persistence; tumor-infiltrating lymphocytes; cancer immunotherapy

Corresponding author: Yong-Chen Lu, Surgery Branch, National Cancer Institute, National Institutes of Health, Building 10-CRC, Rm 3-5930, 10 Center Dr, Bethesda, MD, 20892. Phone: 240-858-3818, Yong-Chen.Lu@nih.gov. **Corresponding author:** Steven A. Rosenberg, Surgery Branch, National Cancer Institute, National Institutes of Health, Building 10-CRC, Rm 3-3940, 10 Center Dr, Bethesda, MD, 20892. Phone: 240-858-3080, sar@nih.gov.

Disclosure of Potential Conflicts of Interest: No potential conflicts of interest were disclosed.

Introduction

Adoptive cell therapy (ACT) using tumor-infiltrating lymphocytes (TILs) has shown significant efficacy in patients with metastatic melanoma (1). Striking responses have been observed in individual patients with metastatic cholangiocarcinoma, cervical cancer, colorectal cancer, or breast cancer after ACT (2–5). However, clinical responses to ACT have been limited in the majority of patients with solid epithelial cancers (3,4,6). To increase the efficacy of the current treatments, multiple aspects of ACT are being explored, including the selection of effective targets and the avidity of antigen-reactive T cells (7,8). Our previous studies have shown that neoantigen recognition by T cells is a major factor associated with effective TIL-ACT (2,9–11). Other studies have also demonstrated that effective immune checkpoint blockade immunotherapies correlate with the abundance of neoantigens expressed by tumors (12–15). Despite efforts to expand and transfer selective TIL populations recognizing neoantigen targets, many of the TIL treatments have been ineffective (6,16).

The persistence of specific T-cell clonotypes in the peripheral blood after T-cell infusion has become an important parameter to monitor during the course of ACT (17). In addition to the antigen avidity of T cells, several factors can also influence T-cell persistence in the peripheral blood. Examples include the levels of homeostatic cytokines, endogenous T-cell reconstitution, tumor antigen expression, and the tumor microenvironment (17–20). Therefore, it is difficult to study persistence data because of many potential variables, unless the analysis is from a large number of patients treated with nearly the same cell product (17).

In a previous study, we observed that patient-4095 with metastatic colorectal cancer, who was treated with mutated *KRAS*(G12D)-reactive TILs, experienced a partial response for 9 months after ACT (4). A single non-responding pulmonary lesion was resected, and the patient has remained disease-free for three years after treatment. We found that the infused TILs comprised three dominant clonotypes (49.5%, 19.1%, 6.9%, respectively). The first clonotype, 9.1-NP, recognized a KRAS(G12D) 9-mer epitope (GADGVGKSA); the second clonotype, 10-P, recognized a KRAS(G12D) 10-mer epitope (GADGVGKSAL); and the third clonotype, 9.2-P, recognized the same 9-mer epitope as 9.1-NP. The most dominant clonotype, 9.1-NP, did not persist (NP) at all on day 40, but the 10-P and 9.2-P clonotypes continued to persist (P) up to day 266 after ACT. The 9.1-NP and 9.2-P clonotypes shared the same specificity and similar TCRα/β sequences, except one amino acid at the CDR3α region and six amino acids at the CDR3β region, and no significant difference in TCR avidity was observed (4).

Because these three clonotypes shared the same *in vitro* culture environment and *in vivo* host environment, we sought to investigate whether different gene expression profiles were associated with different durations of persistence after ACT. Because the majority of biological assays cannot distinguish the difference between 9.1-NP and 9.2-P T cells, we performed single-cell TCR and transcriptome analysis for this single-patient study. The results suggested that TILs that could persist in patient-4095 had distinguishable gene expression profiles, including key genes encoding surface markers and transcription factors.

Materials and Methods

Patients

Patients were enrolled in a clinical trial of TIL therapy (ClinicalTrial.gov ID:). This trial was approved by the institutional-review board (IRB) of the National Cancer Institute (NCI), and the written informed consent was obtained from the patients, following NIH guidelines and Declaration of Helsinki.

The characteristics, treatment, and clinical response for patient-4095 with metastatic colorectal cancer have been published previously (4). We have also reported the summary of characteristics for patient-4007, −4071, and −4081 with metastatic colorectal cancer and patient-4069 with pancreatic cancer (6,16). Briefly, TILs were generated from the metastatic tumors of patients. TIL cultures were selected based on the reactivities against tumor-specific mutations, and selected TIL cultures were expanded for treatment. The patients were treated with a lymphodepleting chemotherapy regimen, a single infusion of TILs, followed by several doses of IL2. The peripheral blood lymphocyte (PBL) samples were obtained from the patients every 2–3 days during hospitalization and during follow-up visits. PBL samples were cryopreserved and stored in a liquid nitrogen container before use. The percentage of individual T-cell clonotypes in samples was obtained by an Immunoseq Assay service, provided by Adaptive Biotechnologies (Seattle, WA).

Generation of TILs

TILs used for this study were generated by methods described previously (21). Briefly, metastatic tumors were resected from patients, and tumor fragments were excised and cultured in RPMI medium supplemented with 10% in-house human AB serum, 2 mM L-glutamine, 25 mM HEPES, gentamicin (10 μg/mL), and IL2 (6000 IU/mL; Clinigen, Yardley, PA). TIL cultures were grown for 2–4 weeks and then screened for recognition of tumor-specific mutations (22). The screening results for patient-4095, −4007, −4071, −4081, and −4069 have been published (4,6,16). The mutation-reactive TIL cultures were selected and expanded using a rapid expansion protocol (REP) to large numbers for patient infusion (23). The REP culture contained 5×10^6 TILs and 5×10^8 irradiated PBMC feeder cells in RPMI/AIM V medium (50%/50% mixed), supplemented with 7.5% in-house human AB serum, 2 mM L-glutamine, IL2 (3000 IU/mL), and OKT3 antibody (30 ng/mL; Miltenyi Biotec, Bergisch Gladbach, Germany) in a G-Rex100 flask (Wilson Wolf, Saint Paul, MN). A small portion of TILs were cryopreserved and stored in a liquid nitrogen container for the experiments shown in this report.

Single-cell TCR/transcriptome sequencing

The samples of infused TILs were thawed and recovered overnight in RPMI/AIM V medium (50%/50%) supplemented with 5% human AB serum (Valley Biomedical, Winchester, VA). TILs were resuspended in PBS and then subjected to a 10X Chromium instrument (10X Genomics, Pleasanton, CA) for the single-cell analysis, as described below. $1X10^7$ PBLs from patient-4095 were stained with KRAS-9mer tetramer or KRAS-10mer tetramer (NIH tetramer core facility, Atlanta, GA), together with CD8 antibody (clone RPA-T8, BD Biosciences, San Jose, CA) for 40 minutes. Stained cells were washed twice with PBS

containing 5% fetal bovine serum (SAFC, St. Louis, MO). After washes, tetramer-positive cells were sorted by BD FACSAria II and subjected to a 10X Chromium instrument for the single-cell analysis.

We used the standard protocol and reagent kit for single-cell V(D)J analysis, provided by 10X Genomics. Up to 8 samples/reactions in 8 channels can be processed simultaneously by a 10X Chromium instrument. Briefly, 10,000 cells per reaction/channel were loaded, with the targeted cell recovery of 6,000 cells. For TIL4095, a total of 4 channels were loaded to obtain the desired number of cells. For patient-4095's PBLs on day 12 after ACT, KRAS-9mer tetramer$^+$ cells were loaded on 3 channels and KRAS-10mer tetramer$^+$ cells were loaded on 1 channel. For patient-4095's PBLs on day 40 after ACT, KRAS-9mer tetramer$^+$ cells and KRAS-10mer tetramer$^+$ cells were loaded on 2 channels each. Single cells were captured and lysed, and mRNA was reverse transcribed to cDNA using the provided reagents (10X Genomics). Single-cell cDNA samples were barcoded and amplified by 12 PCR cycles. The amplified cDNA samples were divided into two fractions for used in two analyses. The first fraction was target-enriched for TCRs (10X Genomics proprietary), and barcoded samples were pooled and sequenced by an Illumina NextSeq 550 sequencer (High Output v2 kit, Read1: 150 b.p., Read2: 150 b.p.). The second fraction was processed for 5' gene expression libraries by following the manufacturer's instruction (10X Genomics). Each channel was processed and sequenced separately by an Illumina NextSeq 550 sequencer (High Output v2 kit, Read1: 26 b.p., Read2: 98 b.p.).

Single-cell samples prepared by Fluidigm C1 systems

TIL4095 (TILs from patient-4095) single cells were processed by two identical Fluidigm C1 systems (Fluidigm, South San Francisco, CA), following the protocol published previously (24). Briefly, the infused TIL sample from patient-4095 was thawed and recovered overnight in RPMI/AIM V medium (50%/50%) supplemented with 5% human AB serum. TILs were stained with KRAS-9mer tetramer or KRAS-10mer tetramer, together with CD8 antibody for 40 minutes. After washes, tetramer-positive cells were sorted by BD FACSAria II and subjected to Fluidigm C1 systems for the single-cell analysis. 12,000 KRAS-9mer tetramer$^+$ cells or KRAS-10mer tetramer$^+$ cells were loaded separately on an IFC plate (Fluidigm). Because of the low-abundance of 9.2-P clonotype, KRAS-9mer tetramer$^+$ cells were loaded on 6 additional IFC plates, and 9.2-P single cells were selected based on the CDR3 sequence information. Single-cell samples were processed by the Fludigm C1 system and barcoded by Nextera XT DNA Library Preparation Kit (Illumina). Single-cell samples were first sequenced by an Illumina MiSeq sequencer (High Output v3 kit, Read1: 250 b.p., Read2: 250 b.p.) to identify CDR3 sequences. Single-cell samples with correct CDR3 sequences (9.1-NP, 9.2-P or 10-P) were sequenced again by an Illumina HiSeq2500 sequencer (Read1: 100 b.p., Read2: 100 b.p.), in order to obtain sufficient sequence information for data analysis.

Single-cell bioinformatics analysis and statistical analysis

Single-cell sequencing data were first processed by Cell Ranger pipelines (v2.1.1)(10X Genomics), in order to obtain T-cell clonotypes and gene expression profiles associated with individual single-cell barcodes. T-cell clonotypes were defined based on TCR Vβ CDR3

nucleotide sequences. Single cells with two different TCR Vβ CDR3 nucleotide sequences were likely doublets and were excluded. Low-quality single cells, with less than 200 detectable genes, were also excluded. Genes with less than 10 read counts, as well as mitochondrial genes, were removed from the subsequent analysis. Non-coding RNA genes were not investigated in this study.

To construct the gene expression matrix for the datasets, we merged all uniquely aligned reads with the same unique molecular identifiers (UMI), cell barcode, and gene annotation in the HDF5 format. The raw single-cell data were then normalized with convolution methods (25). The normalized data were decomposed using randomized principal component analysis (26). The principal components were used to generate t-SNE projections, which were implemented with R package Seurat v.2.3 (https://github.com/satijalab/seurat). The differential expression comparisons were generated with edgeR package with selected genes (false discovery rate, FDR<0.05).

Gene Set Enrichment Analysis

The Persistence_Up and Persistence_Down gene sets were constructed based on the shared, differentially expressed genes (FC > ±1.5, FDR < 0.05), obtained from the comparisons of 9.1-NP vs 9.2-P and 9.1-NP vs 10-P (Supplementary Table S1). Gene Set Enrichment Analysis (GSEA (27)) software/scripts and instruction are publicly available from Broad Institute (http://software.broadinstitute.org/gsea/index.jsp). We made necessary in-house modifications for the scripts, in order to execute the GSEA scripts on the NIH Biowulf server ((http://hpc.nih.gov).

Single-cell bioinformatics analysis for single-cell data obtained by Fluidigm C1 systems

Single-cell whole-transcriptome sequences obtained by the Fluidigm C1 were first analyzed by an in-house bioinformatics pipeline to obtain TCR-CDR3 nucleotide sequences (24). The sequencing data of single cells with correct CDR3 were further analyzed by a bioinformatics pipeline, including the alignment using STAR (v2.4.2) and raw counts by subread (v1.4.6). Good-quality single cells were defined as cells in which more than 1,500 genes were expressed and detected. Individual genes expressed in more than two cells were selected for the subsequent analysis. The gene expression matrix was generated, and the p-values were calculated by the Wilcoxon signed-rank test.

Data availability

The data discussed in this publication have been deposited in NCBI's Gene Expression Omnibus (28) and are accessible through GEO Series accession number GSE136394 (https://www.ncbi.nlm.nih.gov/geo/query/acc.cgi?acc=GSE136394).

Statistical analysis

Statistics for single-cell data and GSEA are described in the above sections.

Results

To study the gene expression profiles of persistent and non-persistent clonotypes, the infused TILs from patient 4095 were subjected to single-cell TCR/transcriptome sample preparation by a 10X Genomics single-cell instrument, followed by next-generation sequencing. Each single cell contained a unique barcode, which could be used to link the gene expression profiles to one of the three dominant clonotypes (9.1-NP, 9.2-P or 10-P), based on their unique TCR-CDR3β sequences. After filtering out single cells with low-quality data, we obtained 9707 single cells from the 9.1-NP clonotype, 1737 single cells from the 9.2-P clonotype and 2771 single cells from the 10-P clonotype for the downstream bioinformatics analysis (Fig. 1A).

Because 9.1-NP and 9.2-P clonotypes recognized exactly the same 9-mer epitope with similar avidity, we first compared the gene expression profiles of single cells from non-persistent 9.1-NP and persistent 9.2-P clonotypes. We identified a total of 472 differentially expressed genes with false discovery rate (FDR) less than 0.05 (Fig. 1B–C; Supplementary Table S2). By comparing the fold changes (FC) of gene expression between 9.1-NP and 9.2-P, we identified the top 10 upregulated genes and the top 10 downregulated genes. These genes are listed in Figure 1D, and these 20 genes are also highlighted in the heatmap and volcano plot (Fig. 1B–C). The brief descriptions of their known functions are listed in Supplementary Table S3, based on the summaries obtained from online databases Genecards (www.genecards.org) and OMIM (www.omim.org). Gene functions in 18 out of the 20 genes have been reported in previous studies, and nine of them have been shown to function significantly in T cells. However, the biological roles of *C1orf162* and *TPRG1* have been largely unknown (Fig. 1D).

We then compared the single-cell gene expression profiles from non-persistent 9.1-NP and persistent 10-P single cells, with the caveat that 10-P clonotype recognized a longer epitope with one additional leucine at the C-terminus. Similarly, a total of 528 differentially expressed genes (FDR<0.05) were identified in this comparison (Fig. 1E–F; Supplementary Table S2). The top 10 upregulated genes and the top 10 downregulated genes based on the FC of gene expression are listed in Figure 1G. These 20 genes are also highlighted in the heatmap and volcano plot (Fig. 1E–F). The brief descriptions of their known functions are listed in Supplementary Table S4. Gene functions in all 20 genes have been reported in previous studies, and nine of them have been shown to function significantly in T cells (Fig. 1G).

By assessing these two sets of differentially expressed genes, a total of 411 genes were shared between these two comparisons (Fig. 2A). A total of 11 genes in the top upregulated and downregulated gene lists were shared between both groups (bold text, Fig. 1D,G). Because these gene signatures were also found in another persistent clonotype 10-P, these genes might be more significant in the biology of persistence than the 61 unique genes in the 9.2-P vs 9.1-NP comparisons. Using the shared 411 genes identified from these two comparisons, a t-distributed stochastic neighbor embedding (t-SNE) plot was generated. The majority of 9.2-P and 10-P single cells were separated from the 9.1-NP single cells (Fig. 2B).

Among these shared gene signatures, we focused on cell surface markers and transcription factors in the top 10 upregulated and downregulated gene lists (Fig. 1D,G). The cell surface markers could be potentially utilized to monitor or enrich T-cell populations associated with the persistence phenotype based on antibody staining, whereas the transcription factors could be the potential key factors defining the persistence phenotype. As shown in Figure 2C, the gene expression of granzyme K (*GZMK*) was much higher in the 9.1-NP non-persistent single cells, compared to the 9.2-P persistent single cells ($\log_2$FC = −3.48, FDR=0). Similarly, the *GZMK* expression was much higher in the 9.1-NP single cells, compared to the 10-P persistent single cells ($\log_2$FC = −3.55, FDR=0)(Fig. 2C). The expression of other granzymes, including *GZMB*, *GZMH*, and *GZMM*, were also significantly higher in the 9.1-NP, compared to the 9.2-P or 10-P single cells (Supplementary Table S2). These results suggested that 9.1-NP single cells showed a more effector-like phenotype, compared to 9.2-P or 10-P single cells. Conversely, NK cell marker KLRB1 (killer cell lectin-like receptor subfamily B, member 1, CD161) had high expression in 9.2-P single cells, compared to 9.1-NP single cells ($\log_2$FC = 3.43, FDR=0) (Fig. 2D). The 10-P single cells were also expressed higher KLRB1 than 9.1-NP single cells, but the difference was less than the 9.1-NP vs. 9.2-P comparison ($\log_2$FC: 3.43 vs. 1.69). The integrin beta 1 (*ITGB1*/CD29) gene also had high expression in both 9.2-P and 10-P single cells, compared to 9.1-NP single cells ($\log_2$FC = 1.97 and 1.83, respectively)(Fig. 2E). In these comparisons, we also found other differentially expressed genes related to T-cell mobility, including integrin *ITGA1* (integrin alpha-1, CD49a), *ITGAX* (integrin alpha X, CD11c), chemokine *CCL3*, *XCL2* and chemokine receptor *CXCR4* and *CCR5* (Supplementary Table S2).

Interleukin-7 (IL7) has been known as one of the master regulators for T-cell homeostasis (20). Higher expression of IL7 receptor (*IL7R*/CD127) was observed in 9.2-P single cells, compared to 9.1-NP single cells ($\log_2$FC = 1.31, FDR=5.19×10^{-73})(Fig. 2F). Similarly, higher *IL7R* expression was observed in 10-P single cells, compared to 9.1-NP single cells ($\log_2$FC = 1.51, FDR = 2.03×10^{-152}). These results suggested that these 9.2-P T cells, as well as 10-P T cells, might be better equipped to compete for the limited resource of IL7, leading to better persistence (20). Sphingosine-1-phosphate receptor 1 (S1PR1) has been described as the predominant receptor for S1P, which is the central mediator of T-cell egress from the thymus or lymphoid organs into the blood (29). The expression of *S1PR1* was higher in 9.2-P single cells, compared to 9.1-NP single cells ($\log_2$FC = 1.22, FDR = 5.38×10^{-72})(Fig. 2G). Similarly, higher *S1PR1* expression was observed in 10-P single cells, compared to 9.1-NP single cells ($\log_2$FC = 1.60, FDR=1.47×10^{-205}). C10orf54, also known as B7H5 or VISTA (the V domain-containing immunoglobulin suppressor of T-cell activation), is one of the B7 family members. Previous studies have suggested that VISTA can negatively regulate T-cell functions in antitumor responses, similar to other checkpoint inhibitors (30). The *C10orf54/VISTA* expression was lower in 9.1-NP single cells, compared to 9.2-P single cells or 10-P single cells ($\log_2$FC = 1.19 and 1.41, respectively)(Fig. 2H). The expression levels of other negative co-stimulatory molecules were low (Supplementary Fig. S1). Cell surface marker CD5 and CD6 have been suggested to negatively regulate TCR signaling, but the evidence for this is not conclusive. *CD5* and *CD6* were both downregulated in both 9.2-P and 10-P single cells, compared to 9.1-NP single cells (Fig. 2I–J).

Several transcription factors were differentially expressed in this analysis, including *ZNF683*, *SOX4*, *CEBPD*, *KLF2* and *EOMES* (Fig. 3A–E; Supplementary Table S2). Zinc finger protein 683 (ZNF683), also known as HOBIT (homolog of BLIMP1 in T cells), has been suggested to serve as a key transcription factor expressed in tissue-resident memory T cells (31). The expression of *ZNF683* was upregulated in 9.2-P single cells, compared to 9.1-NP single cells ($\log_2$FC = 2.71, FDR = 1.92×10^{-119})(Fig. 3A). Similarly, the *ZNF683* expression was upregulated in 10-P single cells, compared to 9.1-NP single cells ($\log_2$FC = 3.97, FDR=0). These results suggested that ZNF683 might also play an important role in T-cell persistence. SOX4 (sex determining region Y-box 4) has been shown to play a key role for CXCL13 production in human $CD4^+$ T cells under inflammatory conditions (32). CCAAT/enhancer binding protein δ (CEBPD) has been known to work synergistically with CEBPB to control the induction of proinflammatory cytokines IL6 and TNFα in macrophages (33). However, its role in T cells is largely unclear. Both *SOX4* and *CEBPD* were downregulated in 9.2-P single cells, compared to 9.1-NP single cells ($\log_2$FC = −1.89 and −1.79, respectively)(Fig. 3B–C). Both *SOX4* and *CEBPD* were also significantly downregulated in 10-P single cells, compared to 9.1-NP single cells ($\log_2$FC = −1.74 and −2.48, respectively).

It has been reported that the transcription factor Klf2 (Kruppel like factor 2) can promote the expression of S1pr1 and restrain the differentiation of $CD4^+$ T follicular helper cells in mice (34). The expression of *KLF2* was higher in 9.2-P single cells, compared to 9.1-NP single cells ($\log_2$FC = 1.15, FDR = 3.94×10^{-69})(Fig. 3D). The *KLF2* expression in 10-P single cells was also higher than 9.1-NP single cells ($\log_2$FC = 1.68, FDR = 7.62×10^{-250}). Lastly, the transcription factor EOMES (eomesodermin) has been identified as one of the key markers among exhausted T-cell populations (35). Significantly less *EOMES* expression was observed in 9.2-P single cells, compared to the 9.1-NP single cells ($\log_2$FC = −0.89, FDR = 3.59×10^{-94})(Fig. 3E). The *EOMES* expression was also significantly downregulated in 10-P single cells, compared to the 9.1-NP single cells ($\log_2$FC = −1.57, FDR=0).

To test whether we could observe the same gene expression patterns using a different approach, we utilized another single-cell system developed by Fluidigm. This system uses a different molecular approach for the single-cell transcriptome analysis. Because Fluidigm C1 is a low-throughput system, TILs were first enriched using the binding of KRAS-9mer or KRAS-10mer tetramer and then subjected to the Fluidigm C1 single-cell system. The full-length, whole-transcriptome sequences from each single cell were obtained, including TCR-CDR3 information for clonotype identification (24). We obtained a total of 123 good-quality single cells from 9.1-NP, 42 single cells from 9.2-P and 72 single cells from 10-P. As illustrated in Figure 2–3, significant differences ($p<0.05$) were observed in 11 of the 13 genes when comparing 9.1-NP vs 9.2-P, except *IL7R* and *KLF2*, possibly due to the low number of cells obtained from 9.2-P single cells from this low-throughput approach (Supplementary Fig. S2). Significant differences were observed in all 13 genes comparing 9.1-NP vs 10-P (Supplementary Fig. S2).

To further observe the gene expression profiles of T cells after ACT, the patient's peripheral blood lymphocytes (PBLs) were stained with KRAS-9mer tetramer or KRAS-10mer tetramer in the attempt to enrich the 9.1-NP, 9.2-P or 10-P populations. The non-persistent

clonotype 9–1-NP was detectable on day 12, but not detectable on day 40 after ACT. Using the methods previously described (Fig. 1A), single-cell samples were prepared from the enriched populations by a 10X Genomics single-cell instrument (Fig. 4A). Using the peripheral blood sample from day 12 after ACT, we obtained a total of 7365, 525, and 3487 good-quality single cells associated with 9.1-NP, 9.2-P and 10-P clonotypes, respectively. From the peripheral blood sample on day 40 after ACT, we acquired a total of 7919 and 5806 good-quality single cells associated with 9.2-P and 10-P clonotypes, respectively. In this analysis, TILs were plotted together with PBLs to observe the changes of gene expression following ACT (Supplementary Table S5).

As previously demonstrated, the 9.2-P and 10-P TILs expressed minimum amounts of *GZMK*, compared to 9.1-NP TILs. On day 12 after cell transfer, significant expression of *GZMK* was observed in the peripheral blood 9.2-P single cells, although the expression was slightly lower than 9.1-NP single cells in PBLs ($\log_2$FC = −0.16, FDR=9.69×10^{-3})(Fig. 4B). On day 40, 9.2-P single cells continued to express a high *GZMK*. Similar observations were found in 10-P single cells, compared to 9.1-NP single cells in the PBLs on day 12 ($\log_2$FC = −1.70, FDR=0). *KLRB1* had high expression in 9.2-P TILs and 10-P TILs. After ACT, 9.2-P T cells in PBLs continued to express high *KLRB1* on day 12 and day 40 (Fig. 4C). However, 10-P T cells lost the expression of *KLRB1* on day 12 after ACT, and 10-P T cells continued to express low *KLRB1* on day 40 (Fig. 4C). Similar to the observation in TILs, *ITGB1* expression was higher in both 9.2-P and 10-P, compared to 9.1-NP on day 12 ($\log_2$FC = 1.12 and 0.96, respectively). For both 9.2-P and 10-P, the *ITGB1* expression was slightly higher on day 40, compared to day 12 ($\log_2$FC = 0.21 and 0.31, respectively)(Fig. 4D). As one of the key regulators for T-cell homeostasis (20), IL7R expression remained higher in 9.2-P single cells, compared to 9.1-NP single cells on day 12 ($\log_2$FC = 0.62, FDR=2.62×10^{-12}). The 9.2-P T cells significantly upregulated *IL7R* on day 40, compared to 9.2-P T cells on day 12 ($\log_2$FC = 1.66, FDR = 6.21×10^{-127}) (Fig. 4E). Similar results were observed in peripheral blood 10-P T cells, compared to 9.1-NP T cells ($\log_2$FC = 0.86, FDR=6.4×10^{-122}). These results suggested that 9.2P and 10-P were more competitive in terms of obtaining limited homeostatic cytokine IL7 *in vivo*. The *S1PR1* expression was not significantly different between peripheral blood 9.1-NP and 9.2-P T cells on day 12, but the *S1PR1* expression was significantly higher in 9.2-P T cells on day 40, compared to 9.2-P T cells on day 12 after ACT ($\log_2$FC = 0.95, FDR = 3.43×10^{-15})(Fig. 4F). On the other hand, the *S1PR1* expression was significantly higher in peripheral blood 10-P T cells, compared to 9.1-NP T cells on day 12 ($\log_2$FC = 0.42, FDR = 8.06×10^{-23}).The *S1PR1* expression was significantly higher in 10-P T cells on day 40, compared to 10-P T cells on day 12 after ACT ($\log_2$FC = 0.83, FDR = 4.55×10^{-65}). The expression of *C10orf54* (*VISTA*) was slightly higher in 9.2-P T cells, compared to 9.1-NP T cells on day 12 after ACT ($\log_2$FC = 0.27, FDR = 1.48×10^{-2})(Fig. 4G). The expression of other negative co-stimulatory molecules were low (Supplementary Fig. S1). Both *CD5* and *CD6* expression was significantly lower in 9.2-P T cells, compared to 9.1-NP T cells on day 12 ($\log_2$FC = −1.23 and −1.24, respectively)(Fig. 4H–I).

Similar to the observation in TILs, the transcription factor *ZNF683* also had high expression in 9.2-P T cells on day 12, compared to 9.1-NP T cells on day 12 ($\log_2$FC = 1.83, FDR = 2.14×10^{-72})(Fig. 5A). Similarly, 10-P T cells expressed higher *ZNF683*, compared to 9.1-

NP T cells on day 12 ($log_2FC = 2.51$, FDR=0). Both 9.2-P and 10-P T cells on day 40 expressed higher *ZNF683*, compared to 9.2-P and 10-P T cells on day 12 ($log_2FC = 0.54$ and 0.61, respectively). The expression of *SOX4* and *CEBPD* was minimum among the peripheral blood 9.1-NP, 9.2-P and 10-P T cells (Fig. 5B–C). The expression of transcription factor *KLF2* was higher in 9.2-P T cells, compared to 9.1-NP T cells in the peripheral blood on day 12 ($log_2FC = 0.34$, FDR=4.97×10^{-4})(Fig. 5D). Similarly, 10-P T cells expressed higher *KLF2* than 9.1-NP T cells on day 12 ($log_2FC = 0.81$, FDR=2.17×10^{-109}). Lower levels of *EOMES* expression were observed in 9.2-P on day 12, compared to 9.1-NP ($log_2FC = -0.49$, FDR = 7.38×10^{-6}). However, the expression of *EOMES* in 9.2-P increased on day 40, compared to day 12 ($log_2FC = 0.26$, FDR = 2.13×10^{-2})(Fig. 5E). Similarly, lower *EOMES* expression was observed in 10-P on day 12, compared to 9.1-NP ($log_2FC = –0.58$, FDR = 3.05×10^{-43}). However, the expression of *EOMES* in 10-P also increased on day 40, compared to day 12 ($log_2FC = 0.18$, FDR = 1.3×10^{-5})(Fig. 5E). Taken together, we observed the continuing high expression of *IL7R*, *ITGB1*, *ZNF683* and *KLF2* in peripheral blood 9.2-P and 10-P T cells following ACT. On the other hand, 9.1-NP T cells had relatively lower expression of these genes in PBLs, compared to 9.2-P or 10-P T cells.

The persistence of T cells can be influenced by the host condition, including the levels of homeostatic cytokines, endogenous T-cell reconstitution, the tumor microenvironment, as well as the binding affinity between TCR and antigen/HLA (17–20). With these caveats in mind, we attempted to test whether or not other infused TILs expressed a set of genes associated with persistence. From the comparisons of 9.1-NP vs 9.2-P and 9.1-NP vs 10-P, 38 shared genes were significantly upregulated, and 41 shared genes were significantly downregulated (FC > ±1.5, FDR<0.05), which were defined as the Persistence_Up gene set and Persistence_Down gene set, respectively (Supplementary Table S1.) To perform the Gene Set Enrichment Analysis (GSEA) analysis (27), we selected four autologous TILs, 4007, 4069, 4071, and 4081, obtained from patients with metastatic gastrointestinal cancers (6,16). These autologous TILs were used to treat these four patients within the five-month window prior to the treatment of patient 4095. The same as the majority of infused TILs in this clinical trial, these four TILs contained predominantly (32.3 ~ 91.9%) neoantigen-reactive $CD8^+$ T cells but persisted poorly one month after ACT (Fig. 6A; Supplementary Table S6)(4,16). Following the same process as the previous experiments, the single-cell transcriptome analysis was performed to study gene expression profiles linked to neoantigen-reactive clonotypes. These single cells associated with neoantigen-reactive clonotypes were first compared to the persistent clonotypes (9.2-P and 10-P), and the differentially expressed genes were subjected to the GSEA analysis. As shown in Figure 6 (B–E), strong differences were observed in all eight GSEA tests for Persistence_Up and Persistence_Down gene sets. Therefore, these TILs obtained from four patients did not express the gene sets associated with the persistence, suggesting that these TILs might lack the “fitness” to persist *in vivo*.

Discussion

In this study, we discovered a gene expression profile associated with T-cell persistence in a patient treated for KRAS(G12D)-expressing tumors. It has been known that IL7 is one of the

key cytokines involved in T-cell homeostasis. (20). It is thus likely that T cells with high IL7R could have a survival advantage over the low IL7R cells. The 9.2-P and 10-P persistent T cells expressed high *IL7R* prior and after ACT, compared to the 9.1-NP non-persistent T cells. Similarly, a previous study suggested that *in vitro* expanded MART1- or gp100-specific T-cell clones that expressed the IL7R were more likely to persist longer after adoptive transfer to patients (36). Next, we studied S1PR1 and KLF2, the key regulators to promote T-cell egress from the thymus or lymphoid organs into the blood (29). A previous mouse study showed that Klf2 could induce the expression of S1pr1 and limit the differentiation of $CD4^+$ T follicular helper cells (34). Another study suggests that $CD8^+$ resident memory T cells express low Klf2 and S1pr1 (37). Consistent with these findings, we found that 9.2-P and 10-P persistent TILs expressed high *KLF2* and *S1PR1*, whereas 9.1-NP non-persistent TILs expressed low *KLF2* and *S1PR1*. After ACT, 9.2-P and 10-P T cells continued to express *KLF2* and *S1PR1*. Because of the limitation in the human study, it is unclear whether or not T cells can downregulate *KLF2* and *S1PR1*, and subsequently enter the tumor.

One of the most significant changes observed in this study was the expression of *ZNF683* in T cells that were infused and persisted. Znf683 (Hobit) was identified as a homolog of Blimp1 and a key transcription factor for $CD8^+$ tissue-resident memory T cells in mice (31). Zundler S *et al* demonstrates that Znf683 and Blimp-1 double-knockout mice are protected in $CD4^+$ tissue-resident, memory T cell-mediated experimental colitis models (38). Conversely, a human study observes that ZNF683 (HOBIT) has high expression in viral-specific $CD8^+$ effector T cells in peripheral blood, and it was proposed that ZNF683 might be a key transcription factor for long-lived effector-type T cells based on this observation (39,40). However, no further evidence has been published to support this hypothesis. In this study, we found that the *ZNF683* expression in the infused $CD8^+$ TILs was associated with their persistence *in vivo*. *ZNF683* was highly expressed in persistent 9.2-P and 10-P T cells in peripheral blood 12 and 40 days after cell infusion. Therefore, ZNF683 might serve as a key transcription factor for T-cell persistence, potentially working together with other transcription factor(s), such as KLF2. Conversely, it is possible that not only a few key transcription factors, but the entire gene expression profile is responsible for the fitness of TILs.

It has been well-established that “younger” T cells, including naïve T cells, stem cell memory T cells, and central memory T cells, can persist better *in vivo* and induce stronger anti-tumor responses, compared to the “older”, terminally differentiated, effector memory T cells (41). However, it is puzzling that terminally differentiated T cells still can induce durable tumor regressions following TIL-ACT or checkpoint immunotherapy. To explain this, it has been proposed that mouse exhausted T cells can be divided into two subsets: (i) “Early” exhaustion subset, defined as $Eomes^{lo}PD\text{-}1^{int}Tcf1^+$ T cells; (ii) “Terminal” exhaustion subset, defined as $Eomes^{hi}PD\text{-}1^{hi}Tbet^{lo}Tcf1^-$ T cells (42). The $Eomes^{hi}$ subset has poor proliferative potential but retains partial cytotoxicity, whereas $Eomes^{lo}$ subset retains moderate proliferative capacity but has limited cytotoxicity (35).The $Eomes^{lo}$ early exhaustion subset can convert to the $Eomes^{hi}$ terminal exhaustion subset after antigen stimulation and proliferation, and this process is not reversible (35). More importantly, PD-1 blockade can reverse and reinvigorate the exhausted phenotype of $Eomes^{lo}$ subset, but not

the Eomes^{hi} subset (43). However, the majority of evidence supporting this hypothesis was obtained from the LCMV chronic infection model, and there is little evidence in human cancer studies to support this hypothesis directly (42). In the present study, the persistent 9.2-P and 10-P TILs had lower *EOMES* expression than the non-persistent 9.1-NP TILs. Similarly, 9.2-P and 10-P TILs also expressed low *GZMK*, known to be associated with cytotoxicity. Following ACT, the persistent 9.2-P and 10-P T cells in the peripheral blood had lower *EOMES* than the non-persistent 9.1-NP T cells, and on day 40, 9.2-P and 10-P T cells upregulated *EOMES*, compared to 9.2-P and 10-P T cells on day 12 after ACT. Therefore, our observation in this study was in line with this hypothesis. However, further evidence is required, such as tracking the T-cell phenotypes in the peripheral blood and tumors through the course of immunotherapy, which can be difficult in human studies. It has also been hypothesized that Tcf1^{+} "memory-like" exhausted T cells are proliferation-competent and responsible for the anti-virus or likely antitumor responses after PD-1 blockade immunotherapy (44–46). However, the expression *TCF1* (*TCF7*) were minimum in our single-cell analysis, and no significant difference of *TCF1* (*TCF7*) expression was observed between 9.1-NP vs 9.2-P or 9.1-NP vs 10-P.

It remains an open question whether or not the persistence of T cells in the peripheral blood is required for tumor regression and clinical responses or is merely a byproduct of vigorous immune responses. Our previous ACT studies using melanoma TILs demonstrate a significant correlation between the persistence of TIL clonotypes and clinical responses (47). Conversely, in another ACT trial using peripheral blood-derived, MART-1-specific cytotoxic T cells, followed by a standard course of anti–CTLA-4, there was no relationship between the persistence of the infused T cells and the tumor responses (48). In ACT studies using CD19 CAR-modified T cells for patients with B-cell leukemias or lymphomas, several studies show the correlation between persistence and responses (17,18,49–52). However, no significant correlation was found in one of the studies (53). In one ACT study using NY-ESO-1 TCR-transduced T cells for patients with synovial sarcoma, a correlation between persistence and clinical responses was observed (54). However, the correlation was not observed in another study for patients with melanoma or synovial sarcoma (55). Taken together, the outcome of ACT is determined by many factors, which may or may not include the persistence of T cells. More direct evidence is needed to further understand these complicated observations.

In summary, we have identified two different TIL populations with distinctive gene expression profiles, which were associated with the persistence of TILs in a patient. Although we could obtain significant knowledge in a relatively defined environment in a single patient, the observation might not be generalized because of the diversity of patients. We plan to do this single-cell analysis for a large number of patients as more patients are accrued in this clinical trial. Given these caveats, the information obtained in this study has opened the possibility to improve TIL therapies against epithelial cancers by enriching TIL populations based on one or the combinations of the cell surface markers, such as KLRB1, ITGB1, IL7R, S1PR1 or C10orf54. Manipulating the expression of key transcription factors, such as ZNF683 and KLF2, may lead to better T-cell products for immunotherapy. These hypotheses need to be further tested in human studies.

Supplementary Material

Refer to Web version on PubMed Central for supplementary material.

Acknowledgements

The authors would like to thank Nicholas Restifo, Steven Shema, Valery Bliskovsky, Michael Kelly and Jinguo Chen for suggestions and technical support. The authors also thank Doug Joubert, NIH Library Writing Center, for manuscript editing assistance. Next-generation sequencing was conducted at the CCR Genomics Core at the National Cancer Institute. This work utilized the computational resources of the NIH HPC Biowulf cluster (http://hpc.nih.gov).

Financial Support: This work was supported by the Intramural Research Program of National Cancer Institute.

References

1. Goff SL, Dudley ME, Citrin DE, Somerville RP, Wunderlich JR, Danforth DN, et al. Randomized, Prospective Evaluation Comparing Intensity of Lymphodepletion Before Adoptive Transfer of Tumor-Infiltrating Lymphocytes for Patients With Metastatic Melanoma. J Clin Oncol 2016;34:2389–97 [PubMed: 27217459]
2. Tran E, Turcotte S, Gros A, Robbins PF, Lu YC, Dudley ME, et al. Cancer immunotherapy based on mutation-specific CD4+ T cells in a patient with epithelial cancer. Science 2014;344:641–5 [PubMed: 24812403]
3. Stevanovic S, Draper LM, Langhan MM, Campbell TE, Kwong ML, Wunderlich JR, et al. Complete regression of metastatic cervical cancer after treatment with human papillomavirus-targeted tumor-infiltrating T cells. J Clin Oncol 2015;33:1543–50 [PubMed: 25823737]
4. Tran E, Robbins PF, Lu YC, Prickett TD, Gartner JJ, Jia L, et al. T-Cell Transfer Therapy Targeting Mutant KRAS in Cancer. N Engl J Med 2016;375:2255–62 [PubMed: 27959684]
5. Zacharakis N, Chinnasamy H, Black M, Xu H, Lu YC, Zheng Z, et al. Immune recognition of somatic mutations leading to complete durable regression in metastatic breast cancer. Nature medicine 2018;24:724–30
6. Parkhurst MR, Robbins PF, Tran E, Prickett TD, Gartner JJ, Jia L, et al. Unique Neoantigens Arise from Somatic Mutations in Patients with Gastrointestinal Cancers. Cancer Discov 2019
7. Tran E, Robbins PF, Rosenberg SA. 'Final common pathway' of human cancer immunotherapy: targeting random somatic mutations. Nat Immunol 2017;18:255–62 [PubMed: 28198830]
8. Lu YC, Robbins PF. Cancer immunotherapy targeting neoantigens. Semin Immunol 2016;28:22–7 [PubMed: 26653770]
9. Lu YC, Yao X, Li YF, El-Gamil M, Dudley ME, Yang JC, et al. Mutated PPP1R3B Is Recognized by T Cells Used To Treat a Melanoma Patient Who Experienced a Durable Complete Tumor Regression. J Immunol 2013;190:6034–42 [PubMed: 23690473]
10. Robbins PF, Lu YC, El-Gamil M, Li YF, Gross C, Gartner J, et al. Mining exomic sequencing data to identify mutated antigens recognized by adoptively transferred tumor-reactive T cells. Nat Med 2013;19:747–52 [PubMed: 23644516]
11. Schumacher TN, Scheper W, Kvistborg P. Cancer Neoantigens. Annu Rev Immunol 2018
12. Snyder A, Makarov V, Merghoub T, Yuan J, Zaretsky JM, Desrichard A, et al. Genetic basis for clinical response to CTLA-4 blockade in melanoma. N Engl J Med 2014;371:2189–99 [PubMed: 25409260]
13. Van Allen EM, Miao D, Schilling B, Shukla SA, Blank C, Zimmer L, et al. Genomic correlates of response to CTLA-4 blockade in metastatic melanoma. Science 2015;350:207–11 [PubMed: 26359337]
14. Rizvi NA, Hellmann MD, Snyder A, Kvistborg P, Makarov V, Havel JJ, et al. Cancer immunology. Mutational landscape determines sensitivity to PD-1 blockade in non-small cell lung cancer. Science 2015;348:124–8 [PubMed: 25765070]

15. Ribas A, Wolchok JD. Cancer immunotherapy using checkpoint blockade. Science 2018;359:1350–5 [PubMed: 29567705]
16. Tran E, Ahmadzadeh M, Lu YC, Gros A, Turcotte S, Robbins PF, et al. Immunogenicity of somatic mutations in human gastrointestinal cancers. Science 2015;350:1387–90 [PubMed: 26516200]
17. Mueller KT, Maude SL, Porter DL, Frey N, Wood P, Han X, et al. Cellular kinetics of CTL019 in relapsed/refractory B-cell acute lymphoblastic leukemia and chronic lymphocytic leukemia. Blood 2017;130:2317–25 [PubMed: 28935694]
18. Fraietta JA, Lacey SF, Orlando EJ, Pruteanu-Malinici I, Gohil M, Lundh S, et al. Determinants of response and resistance to CD19 chimeric antigen receptor (CAR) T cell therapy of chronic lymphocytic leukemia. Nat Med 2018;24:563–71 [PubMed: 29713085]
19. Martinez M, Moon EK. CAR T Cells for Solid Tumors: New Strategies for Finding, Infiltrating, and Surviving in the Tumor Microenvironment. Front Immunol 2019;10:128 [PubMed: 30804938]
20. Mazzucchelli R, Durum SK. Interleukin-7 receptor expression: intelligent design. Nat Rev Immunol 2007;7:144–54 [PubMed: 17259970]
21. Dudley ME, Wunderlich JR, Shelton TE, Even J, Rosenberg SA. Generation of tumor-infiltrating lymphocyte cultures for use in adoptive transfer therapy for melanoma patients. J Immunother 2003;26:332–42 [PubMed: 12843795]
22. Lu YC, Yao X, Crystal JS, Li YF, El-Gamil M, Gross C, et al. Efficient identification of mutated cancer antigens recognized by T cells associated with durable tumor regressions. Clin Cancer Res 2014;20:3401–10 [PubMed: 24987109]
23. Riddell SR, Watanabe KS, Goodrich JM, Li CR, Agha ME, Greenberg PD. Restoration of viral immunity in immunodeficient humans by the adoptive transfer of T cell clones. Science 1992;257:238–41 [PubMed: 1352912]
24. Lu YC, Zheng Z, Robbins PF, Tran E, Prickett TD, Gartner JJ, et al. An Efficient Single-Cell RNA-Seq Approach to Identify Neoantigen-Specific T Cell Receptors. Mol Ther 2018;26:379–89 [PubMed: 29174843]
25. Lun AT, Bach K, Marioni JC. Pooling across cells to normalize single-cell RNA sequencing data with many zero counts. Genome Biol 2016;17:75 [PubMed: 27122128]
26. Halko N, Martinsson PG, Tropp JA. Finding Structure with Randomness: Probabilistic Algorithms for Constructing Approximate Matrix Decompositions. Siam Rev 2011;53:217–88
27. Subramanian A, Tamayo P, Mootha VK, Mukherjee S, Ebert BL, Gillette MA, et al. Gene set enrichment analysis: a knowledge-based approach for interpreting genome-wide expression profiles. Proc Natl Acad Sci U S A 2005;102:15545–50 [PubMed: 16199517]
28. Edgar R, Domrachev M, Lash AE. Gene Expression Omnibus: NCBI gene expression and hybridization array data repository. Nucleic Acids Res 2002;30:207–10 [PubMed: 11752295]
29. Cyster JG, Schwab SR. Sphingosine-1-phosphate and lymphocyte egress from lymphoid organs. Annu Rev Immunol 2012;30:69–94 [PubMed: 22149932]
30. Lines JL, Sempere LF, Broughton T, Wang L, Noelle R. VISTA is a novel broad-spectrum negative checkpoint regulator for cancer immunotherapy. Cancer Immunol Res 2014;2:510–7 [PubMed: 24894088]
31. Mackay LK, Minnich M, Kragten NA, Liao Y, Nota B, Seillet C, et al. Hobit and Blimp1 instruct a universal transcriptional program of tissue residency in lymphocytes. Science 2016;352:459–63 [PubMed: 27102484]
32. Yoshitomi H, Kobayashi S, Miyagawa-Hayashino A, Okahata A, Doi K, Nishitani K, et al. Human Sox4 facilitates the development of CXCL13-producing helper T cells in inflammatory environments. Nat Commun 2018;9:3762 [PubMed: 30232328]
33. Tsukada J, Yoshida Y, Kominato Y, Auron PE. The CCAAT/enhancer (C/EBP) family of basic-leucine zipper (bZIP) transcription factors is a multifaceted highly-regulated system for gene regulation. Cytokine 2011;54:6–19 [PubMed: 21257317]
34. Lee JY, Skon CN, Lee YJ, Oh S, Taylor JJ, Malhotra D, et al. The transcription factor KLF2 restrains CD4(+) T follicular helper cell differentiation. Immunity 2015;42:252–64 [PubMed: 25692701]

35. Paley MA, Kroy DC, Odorizzi PM, Johnnidis JB, Dolfi DV, Barnett BE, et al. Progenitor and terminal subsets of CD8+ T cells cooperate to contain chronic viral infection. Science 2012;338:1220–5 [PubMed: 23197535]
36. Chandran SS, Paria BC, Srivastava AK, Rothermel LD, Stephens DJ, Kammula US. Tumor-Specific Effector CD8+ T Cells That Can Establish Immunological Memory in Humans after Adoptive Transfer Are Marked by Expression of IL7 Receptor and c-myc. Cancer Res 2015;75:3216–26 [PubMed: 26100671]
37. Skon CN, Lee JY, Anderson KG, Masopust D, Hogquist KA, Jameson SC. Transcriptional downregulation of S1pr1 is required for the establishment of resident memory CD8+ T cells. Nat Immunol 2013;14:1285–93 [PubMed: 24162775]
38. Zundler S, Becker E, Spocinska M, Slawik M, Parga-Vidal L, Stark R, et al. Hobit- and Blimp-1-driven CD4(+) tissue-resident memory T cells control chronic intestinal inflammation. Nat Immunol 2019;20:288–300 [PubMed: 30692620]
39. Vieira Braga FA, Hertoghs KM, Kragten NA, Doody GM, Barnes NA, Remmerswaal EB, et al. Blimp-1 homolog Hobit identifies effector-type lymphocytes in humans. Eur J Immunol 2015;45:2945–58 [PubMed: 26179882]
40. Braun J, Frentsch M, Thiel A. Hobit and human effector T-cell differentiation: The beginning of a long journey. Eur J Immunol 2015;45:2762–5 [PubMed: 26440905]
41. Restifo NP, Dudley ME, Rosenberg SA. Adoptive immunotherapy for cancer: harnessing the T cell response. Nat Rev Immunol 2012;12:269–81 [PubMed: 22437939]
42. McLane LM, Abdel-Hakeem MS, Wherry EJ. CD8 T Cell Exhaustion During Chronic Viral Infection and Cancer. Annu Rev Immunol 2019
43. Blackburn SD, Shin H, Freeman GJ, Wherry EJ. Selective expansion of a subset of exhausted CD8 T cells by alphaPD-L1 blockade. Proc Natl Acad Sci U S A 2008;105:15016–21 [PubMed: 18809920]
44. Wu T, Ji Y, Moseman EA, Xu HC, Manglani M, Kirby M, et al. The TCF1-Bcl6 axis counteracts type I interferon to repress exhaustion and maintain T cell stemness. Sci Immunol 2016;1
45. Im SJ, Hashimoto M, Gerner MY, Lee J, Kissick HT, Burger MC, et al. Defining CD8+ T cells that provide the proliferative burst after PD-1 therapy. Nature 2016;537:417–21 [PubMed: 27501248]
46. Henning AN, Roychoudhuri R, Restifo NP. Epigenetic control of CD8(+) T cell differentiation. Nat Rev Immunol 2018;18:340–56 [PubMed: 29379213]
47. Rosenberg SA, Yang JC, Sherry RM, Kammula US, Hughes MS, Phan GQ, et al. Durable complete responses in heavily pretreated patients with metastatic melanoma using T-cell transfer immunotherapy. Clin Cancer Res 2011;17:4550–7 [PubMed: 21498393]
48. Chapuis AG, Roberts IM, Thompson JA, Margolin KA, Bhatia S, Lee SM, et al. T-Cell Therapy Using Interleukin-21-Primed Cytotoxic T-Cell Lymphocytes Combined With Cytotoxic T-Cell Lymphocyte Antigen-4 Blockade Results in Long-Term Cell Persistence and Durable Tumor Regression. J Clin Oncol 2016;34:3787–95 [PubMed: 27269940]
49. Porter DL, Hwang WT, Frey NV, Lacey SF, Shaw PA, Loren AW, et al. Chimeric antigen receptor T cells persist and induce sustained remissions in relapsed refractory chronic lymphocytic leukemia. Sci Transl Med 2015;7:303ra139
50. Lee DW, Kochenderfer JN, Stetler-Stevenson M, Cui YK, Delbrook C, Feldman SA, et al. T cells expressing CD19 chimeric antigen receptors for acute lymphoblastic leukaemia in children and young adults: a phase 1 dose-escalation trial. Lancet 2015;385:517–28 [PubMed: 25319501]
51. Kochenderfer JN, Somerville RPT, Lu T, Shi V, Bot A, Rossi J, et al. Lymphoma Remissions Caused by Anti-CD19 Chimeric Antigen Receptor T Cells Are Associated With High Serum Interleukin-15 Levels. J Clin Oncol 2017;35:1803–13 [PubMed: 28291388]
52. Park JH, Riviere I, Gonen M, Wang X, Senechal B, Curran KJ, et al. Long-Term Follow-up of CD19 CAR Therapy in Acute Lymphoblastic Leukemia. N Engl J Med 2018;378:449–59 [PubMed: 29385376]
53. Schuster SJ, Svoboda J, Chong EA, Nasta SD, Mato AR, Anak O, et al. Chimeric Antigen Receptor T Cells in Refractory B-Cell Lymphomas. N Engl J Med 2017;377:2545–54 [PubMed: 29226764]

54. D'Angelo SP, Melchiori L, Merchant MS, Bernstein D, Glod J, Kaplan R, et al. Antitumor Activity Associated with Prolonged Persistence of Adoptively Transferred NY-ESO-1 (c259)T Cells in Synovial Sarcoma. Cancer Discov 2018;8:944–57 [PubMed: 29891538]

55. Robbins PF, Kassim SH, Tran TL, Crystal JS, Morgan RA, Feldman SA, et al. A pilot trial using lymphocytes genetically engineered with an NY-ESO-1-reactive T-cell receptor: long-term follow-up and correlates with response. Clin Cancer Res 2015;21:1019–27 [PubMed: 25538264]

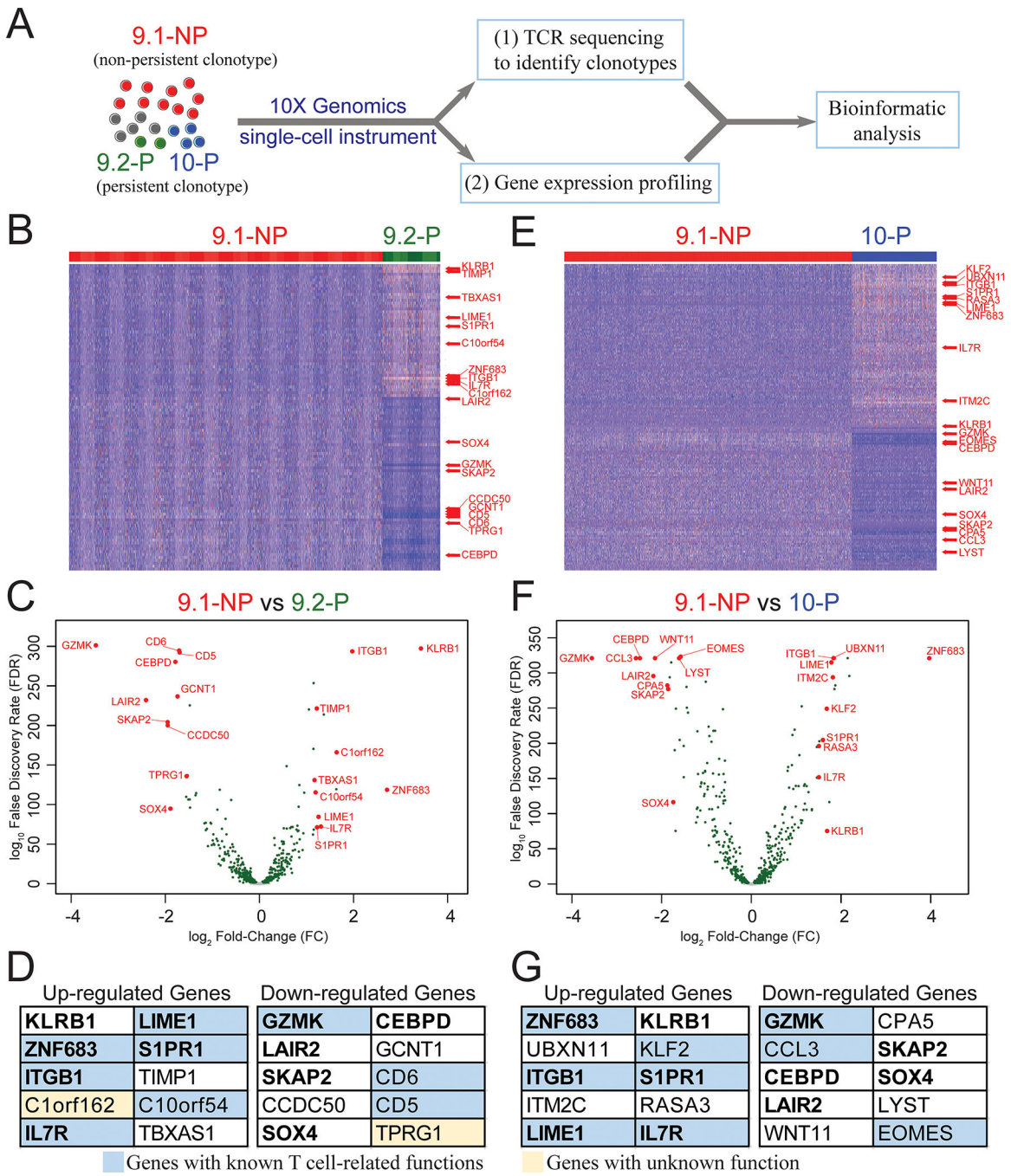

Up-regulated Genes		Down-regulated Genes	
KLRB1	**LIME1**	**GZMK**	**CEBPD**
ZNF683	**S1PR1**	**LAIR2**	GCNT1
ITGB1	TIMP1	**SKAP2**	CD6
C1orf162	C10orf54	CCDC50	CD5
IL7R	TBXAS1	**SOX4**	TPRG1

Up-regulated Genes		Down-regulated Genes	
ZNF683	**KLRB1**	**GZMK**	CPA5
UBXN11	KLF2	CCL3	**SKAP2**
ITGB1	**S1PR1**	**CEBPD**	**SOX4**
ITM2C	RASA3	**LAIR2**	LYST
LIME1	**IL7R**	WNT11	EOMES

Figure 1. Persistent 9.2-P and 10-P single cells showed different gene expression profiles compared to the non-persistent 9.1-NP single cells.

A, TIL4095, contained three dominant clonotypes 9.1-NP, 9.2-P and 10-P (4). TIL4095 T cells were subjected to a single-cell instrument (10X Genomics) to perform (i) single-cell TCR sequencing and (ii) single-cell gene expression profiling. Each single cell contained a unique barcode, which could be used to link the gene expression profiles to one of the three dominant clonotypes (9.1-NP, 9.2-P or 10-P), based on their unique TCR-CDR3β sequences. This set of information was used in the subsequent analysis. Next, single cells from 9.1-NP

non-persistent clonotype were compared with single cells from 9.2-P persistent clonotype to generate **(B)** a heatmap and **(C)** a volcano plot. **(D)** Top 10 upregulated genes and top 10 downregulated genes based on the fold changes (FC) are listed. Genes with known T cell-related functions are shown in blue boxes. Genes with unknown function are shown in yellow boxes. Single cells from 9.1-NP non-persistent clonotype were then compared with single cells from 10-P persistent clonotype to generate **(E)** a heatmap and **(F)** a volcano plot. **(G)** Top 10 upregulated genes and top 10 downregulated genes based on the FC are listed. Genes with known T cell-related functions are shown in blue boxes. For the heatmaps, each vertical line represents a single cell. Only genes with FC>1.5 and false discovery rate (FDR)<0.05 are shown. For the volcano plots, genes with FDR<0.05 are shown in green. The eleven genes shared between (D) and (G) are in bold text.

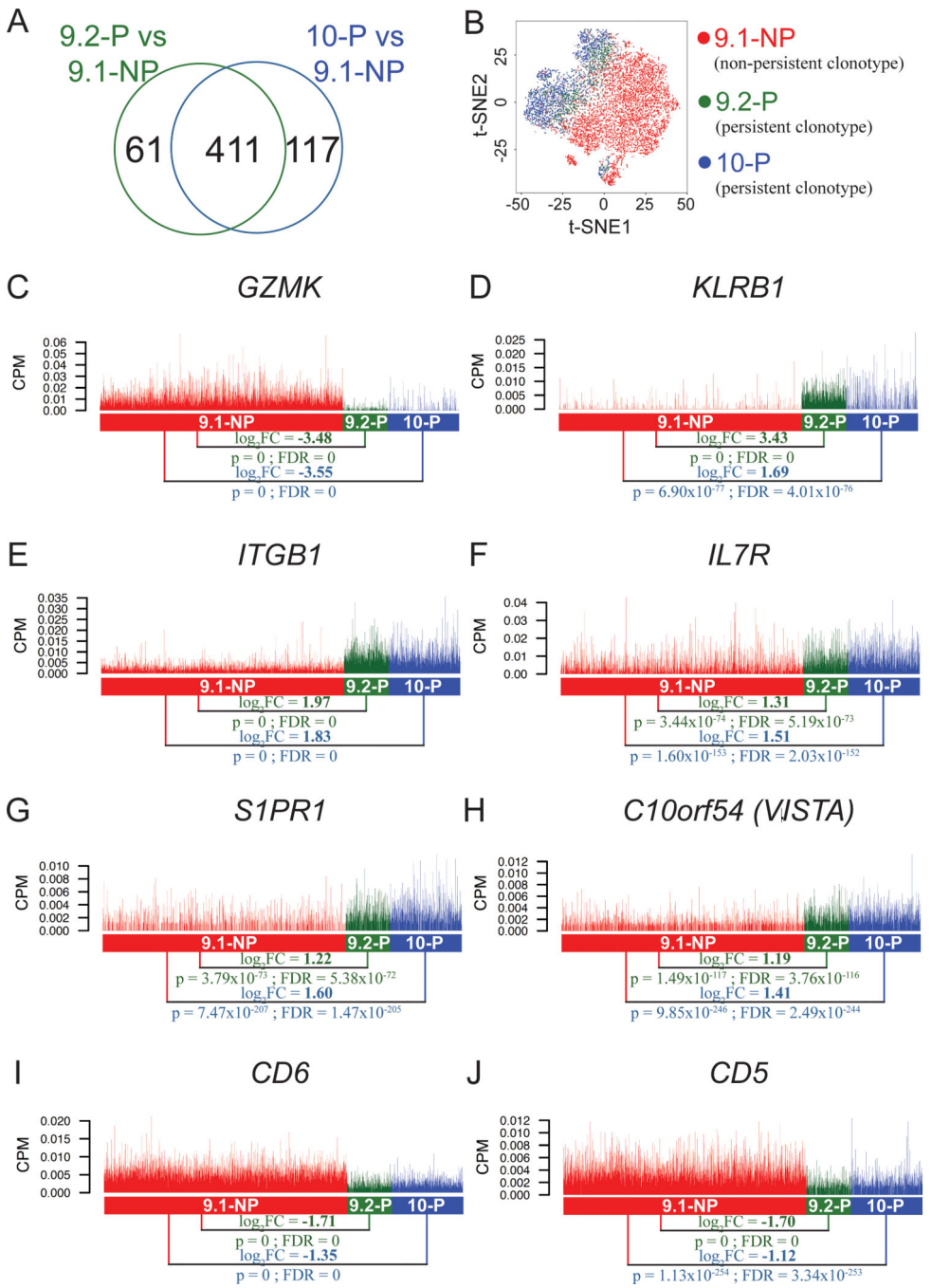

Figure 2. Differentially expressed genes encoding cell surface markers identified in the single-cell transcriptome analysis.

A, Venn diagram showing a total of 472 genes that were differentially expressed (FDR<0.05) in the comparison between 9.1-NP vs. 9.2-P single cells, and a total of 528 genes that were differentially expressed (FDR<0.05) in the comparison between 9.1-NP vs 10-P single cells. Among these genes, a total of 411 genes were shared in these two comparisons. **B,** The t-distributed stochastic neighbor embedding (t-SNE) plot of 9.1-NP, 9.2-P and 10-P single cells using the shared 411 genes obtained from the two comparisons.

C-J, The expression of genes encoding cell surface markers are shown. Each vertical line represents a single cell. CPM: counts per million; GZMK: granzyme K; KLRB1: killer cell lectin like receptor B1; ITGB1: integrin subunit beta 1; IL7R: interleukin 7 receptor; S1PR1: sphingosine-1-phosphate receptor 1; C10orf54 (VISTA): chromosome 10 open reading frame 54 (the V domain-containing immunoglobulin suppressor of T-cell activation).

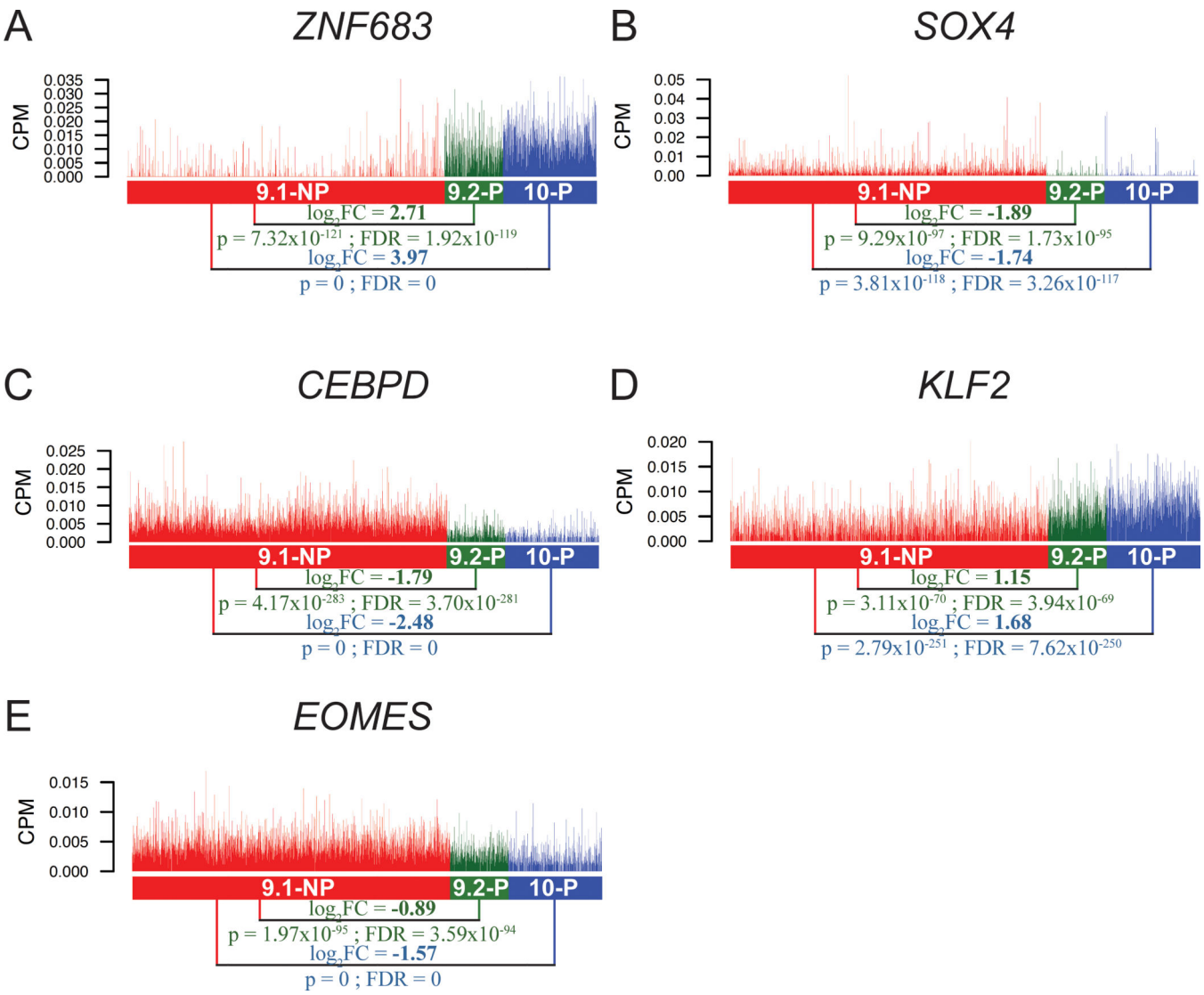

Figure 3. Differentially expressed genes encoding transcription factors identified in the single-cell transcriptome analysis.

A-E, The expression of genes encoding transcription factors are shown. Each vertical line represents a single cell. ZNF683: zinc finger protein 683; SOX4: sex determining region Y-box 4; CEBPD: CCAAT/enhancer binding protein δ; KLF2: Kruppel like factor 2; EOMES: eomesodermin.

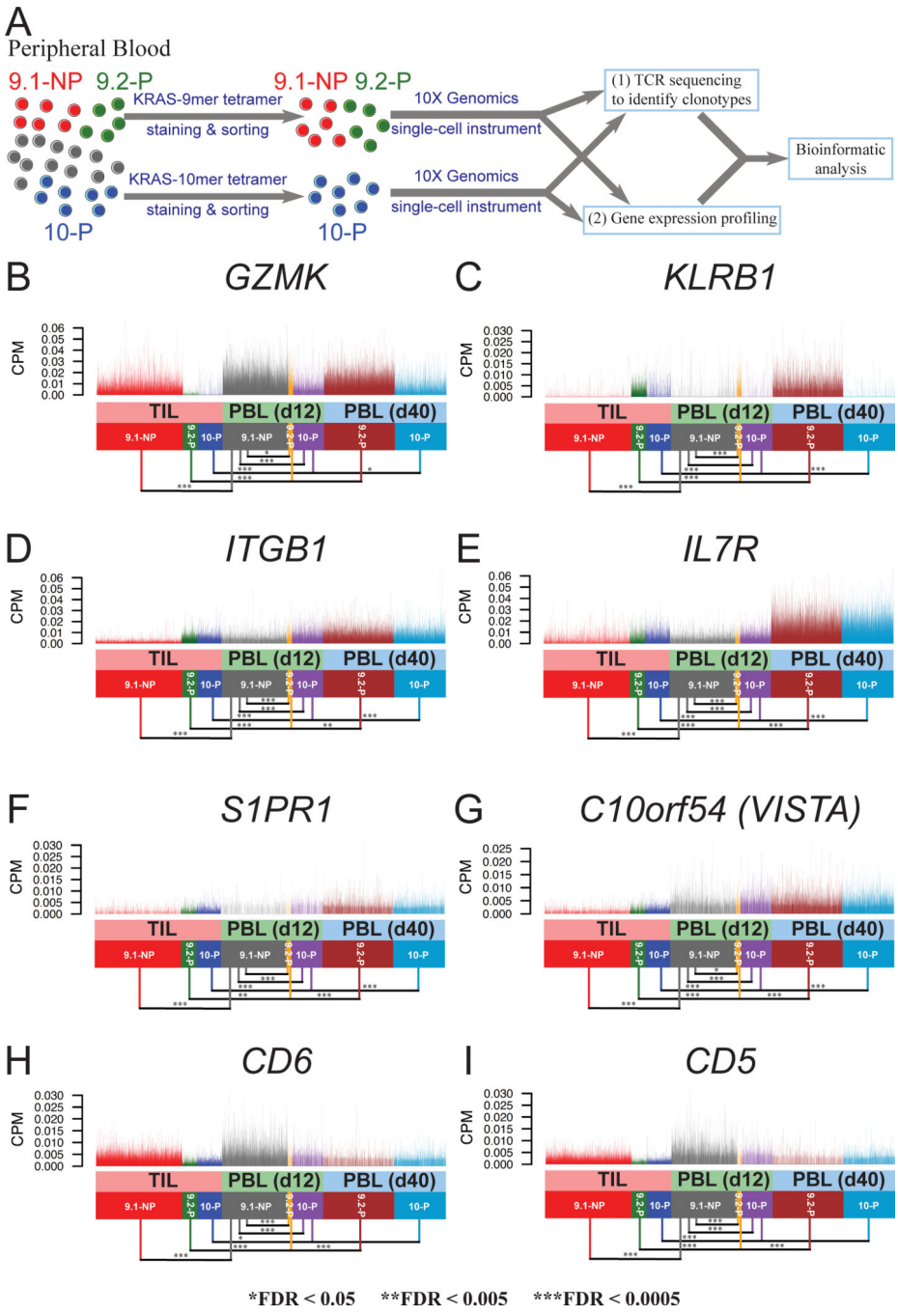

Figure 4. The gene expression of cell surface markers in 9.1-NP, 9.2-P and 10-P single cells isolated from the peripheral blood following ACT.

A, PBL samples on day 12 (d12) and day 40 (d40) were enriched by tetramer staining and sorting, followed by single-cell transcriptome analysis. **B-I,** The expression of genes encoding cell surface markers are shown. Single cells from TILs are plotted together with PBL samples on day 12 and day 40. Each vertical line represents a single cell.

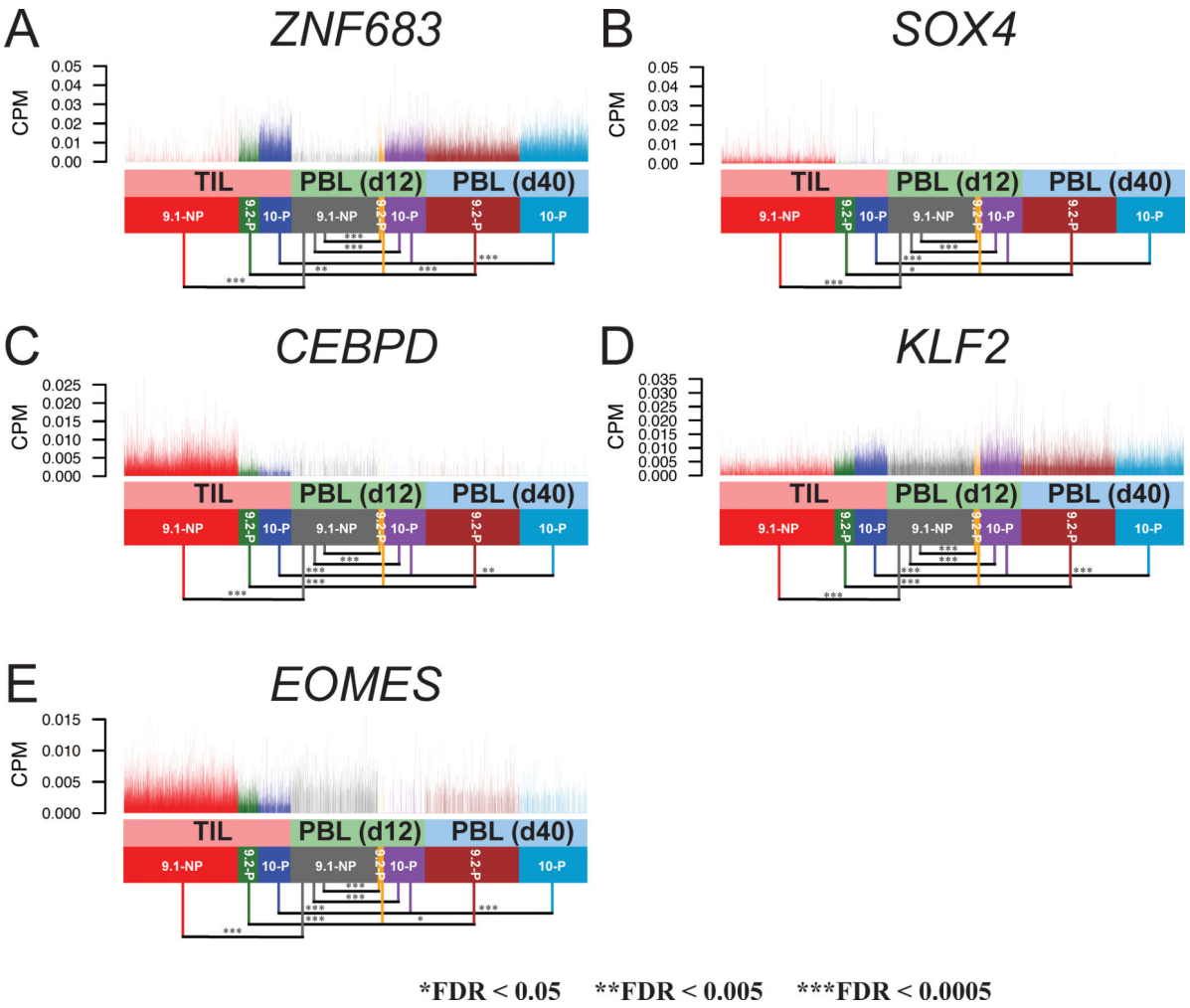

Figure 5. The gene expression of transcription factors in 9.1-NP, 9.2-P and 10-P single cells isolated from the peripheral blood following ACT.

A-E, The expression of genes encoding transcription factors are shown. Single cells from TILs are plotted together with PBL samples on day 12 and day 40. Each vertical line represents a single cell.

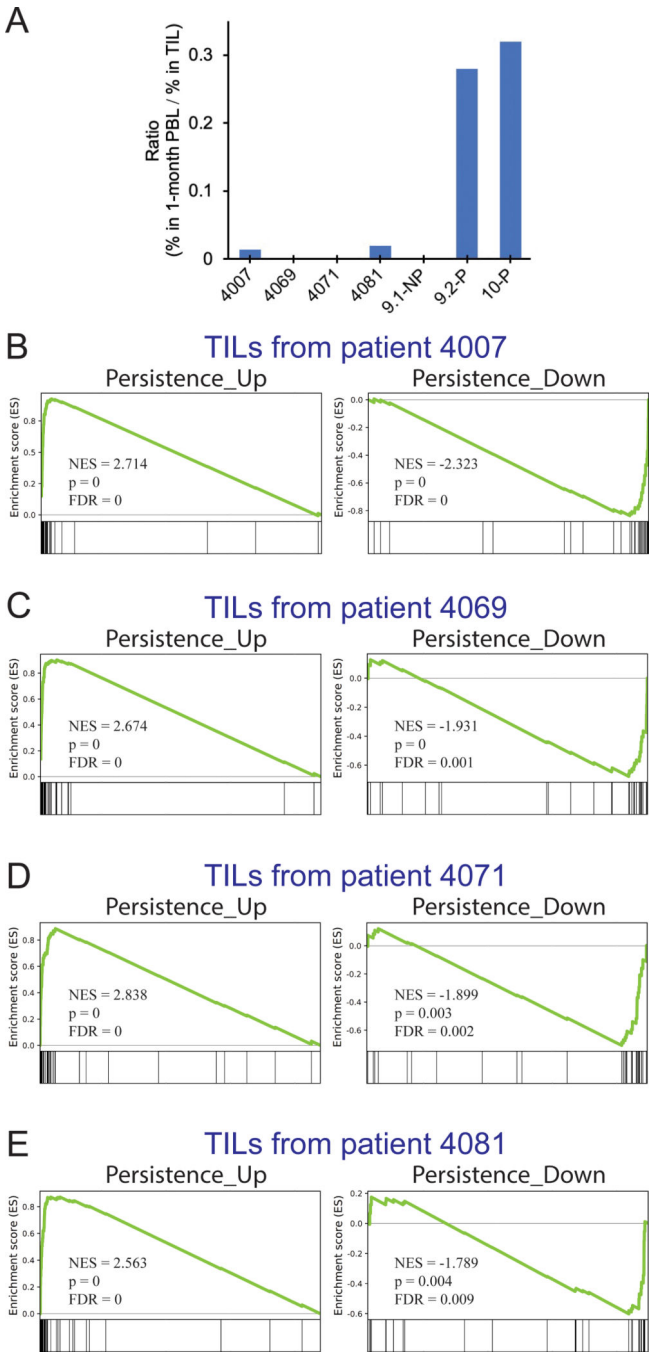

Figure 6. The persistent clonotypes of TIL4095 had different gene expression profile compared to autologous TILs from four gastrointestinal cancer patients.

A, Four patients with metastatic gastrointestinal cancers, 4007, 4069, 4071 and 4081, were treated with autologous TILs within the five-month window prior to the treatment of patient 4095. The ratio of persistence was calculated based on the percentage of neoantigen-specific T cells in PBLs at approximately one month after ACT, divided by the percentage of neoantigen-specific T cells in the infused TILs (Supplementary Table S6). **B-E,** Gene set enrichment analysis (GSEA) was performed to compare 4095 persistent clonotypes (9.2-P

and 10-P) with TIL products from the four patients. Two gene sets, Persistance_Up and Persistance_Down, were used in the GSEA analysis. The Persistence_Up and Persistence_Down gene sets were constructed based on the shared, differentially expressed genes (FC > ±1.5, FDR<0.05), obtained from the comparisons of 9.1-NP vs 9.2-P and 9.1-NP vs 10-P (Supplementary Table S1). NES: normalized enrichment score.